Journal of Zhejiang University SCIENCE A
ISSN 1673-565X (Print); ISSN 1862-1775 (Online)
www.zju.edu.cn/jzus; www.springerlink.com
E-mail: jzus@zju.edu.cn

Modeling of sensor function for piezoelectric bender elements*

Yan-guo ZHOU†, Yun-min CHEN†‡, Hao-jiang DING, Wei-qiu CHEN

(*Key Laboratory of Soft Soils and Geoenvironmental Engineering, Ministry of Education, Zhejiang University, Hangzhou 310027, China*)

†E-mail: qzking@zju.edu.cn; chenyunmin@zju.edu.cn

Received Oct. 10, 2007; revision accepted Nov. 1, 2007; published online Nov. 21, 2007

Abstract: An analytical sandwich beam model for piezoelectric bender elements is derived based on the first-order shear deformation theory (FSDT), which assumes a single rotation angle for the whole cross-section and a quadratic distribution for coupled electric potential in piezoelectric layers. Shear coefficient is introduced to correct the effect of transverse shear strain on shear force and the electric displacement integration. Static and free vibration analyses of simply-supported bender elements are carried out for the sensor function. The results illustrate the high accuracy of the present model compared with the exact 2D solutions.

Key words: Bender elements, Piezoelectric, Sensor, Sandwich beam, Shear coefficient
doi:10.1631/jzus.A071544 **Document code:** A **CLC number:** O34; TU4

INTRODUCTION

Piezoelectric bender element is one of the typical electromechanical transducers, which is capable of converting mechanical energy to electrical energy and vise versa. In the field of soil mechanics and geotechnical engineering, bender elements offer a convenient approach for determining shear wave velocities of soil sediments (Leong *et al.*, 2005). In laboratory, bender elements (actuator and sensor) are cantilever fixed; shear waves triggered by the transmitter (i.e., actuator) propagate through soil sample to the receiver (i.e., sensor), and the arrival of shear waves is judged by the output electric signal of the receiver. Although bender elements are widely used nowadays (Zhou and Chen, 2005; 2007), there are considerable errors in the travel time determination (Arulnathan *et al.*, 1998), which is partly attributed to the lack of understanding of the electromechanical responses of bender elements, especially that of the receiver. Therefore, the study of sensor function of bender elements is important to the interpretation of bender element testing.

Usually, bender element consists of two thin piezoceramic elements glued on each side of a conductive metal shim, a typical so-called piezoelectric sandwich structure. There are two types of bender elements: the series type and the parallel type (Lee and Santamarina, 2005). In the series type, the poling directions of the two piezoelectric layers are opposite each other and the bender element is connected at the outer electrodes as shown in Fig.1a. In the parallel type, the two piezoelectric layers have the same poling direction as shown in Fig.1b, both outer electrodes are grounded, and the core wire is connected to the metal shim.

Unfortunately, until now there are no exact solutions to dynamic problems of such type of piezoelectric cantilever beams, and most of the vibration analyses for similar structures were carried out based on simplified models (Fernandes and Pouget, 2003; Lau *et al.*, 2005; Zhou *et al.*, 2005a; 2005b; 2007). Based on the first-order shear deformation theory (FSDT), this paper established an analytical sandwich beam model for piezoelectric bender elements with thick piezoelectric layers. Static and free vibration analyses of simply supported bender elements were carried out for the sensor function, and the numerical

‡ Corresponding author
* Project supported by the National Natural Science Foundation of China (No. 10472102) and the National Basic Research Program (973) of China (No. 2007CB714200)

results validated the efficiency of the present model by comparison with the exact 2D solutions. Since the forced vibration analysis could be readily obtained by mode superposition based on free vibration solutions, the present work forms a solid base for the sensor function analysis of bender elements.

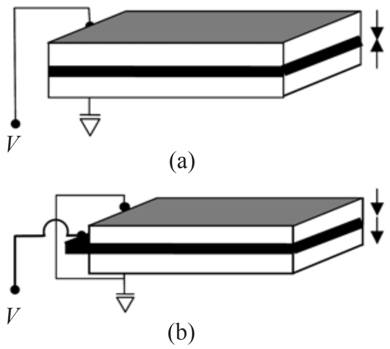

Fig.1 Piezoelectric bender elements
(a) Series type; (b) Parallel type

BASIC EQUATIONS

For orthotropic piezoelectric layers in bender elements, when a plane stress beam is considered in the *x*-*z* plane ($\sigma_y=\tau_{xy}=\tau_{yz}=0$, $D_y=0$), the fundamental equations can be reduced from 2D piezoelasticity (Ding *et al.*, 1997) by further omitting the transverse normal stress ($\sigma_z=0$) as follows:

$$\begin{aligned}&\frac{\partial\sigma_x}{\partial x}+\frac{\partial\tau_{xz}}{\partial z}+f_x=\rho\frac{\partial^2 u_x}{\partial t^2},\\&\frac{\partial\tau_{xz}}{\partial x}+f_z=\rho\frac{\partial^2 u_z}{\partial t^2},\quad \frac{\partial D_x}{\partial x}+\frac{\partial D_z}{\partial z}=0,\end{aligned}\tag{1}$$

$$\sigma_x=\tilde{c}_{11}\varepsilon_x+(-1)^i\tilde{e}_{31}\frac{\partial\phi}{\partial z},\ \tau_{xz}=c_{55}\gamma_{xz}+(-1)^i e_{15}\frac{\partial\phi}{\partial x},\tag{2}$$

$$D_z=(-1)^i\tilde{e}_{31}\varepsilon_x-\tilde{\varepsilon}_{33}\frac{\partial\phi}{\partial z},\ D_x=(-1)^i e_{15}\gamma_{xz}-\varepsilon_{11}\frac{\partial\phi}{\partial x},\tag{3}$$

where σ_x (τ_{xz}), u_x (u_z), D_x (D_z) and ϕ represent the stress components, displacement components, electric displacement components and electric potential; $\tilde{c}_{11}$, $\tilde{\varepsilon}_{33}$ and $\tilde{e}_{31}$ are reduced modulus, piezoelectric constant and dielectric constant, respectively.

$$\begin{aligned}&\tilde{c}_{11}=c_{11}-\frac{c_{12}^2}{c_{22}}-\frac{(c_{13}c_{22}-c_{12}c_{23})^2}{c_{22}(c_{22}c_{33}-c_{23}^2)},\\&\tilde{\varepsilon}_{33}=\varepsilon_{33}+\frac{e_{32}^2}{c_{22}}+\frac{(c_{22}e_{33}-c_{23}e_{32})^2}{c_{22}(c_{22}c_{33}-c_{23}^2)},\\&\tilde{e}_{31}=e_{31}-\frac{c_{12}e_{32}}{c_{22}}-\frac{(c_{13}c_{22}-c_{12}c_{23})(c_{22}e_{33}-c_{23}e_{32})}{c_{22}(c_{22}c_{33}-c_{23}^2)}.\end{aligned}\tag{4}$$

In Eqs.(2) and (3), *i* is an integer representative of poling direction in the piezoelectric layer. $i=2$ when the poling direction coincides with the positive *z* coordinate, and $i=1$ otherwise. Without losing generality, we assume the poling direction of the upper layer is always the same as the positive *z* coordinate.

For the elastic metal layer, the governing equations can be deduced from Eqs.(1) and (2) by omitting the third equation of Eq.(1) and assuming $\tilde{e}_{31}=e_{15}=0$ in Eq.(2). Furthermore, one may assume $\tilde{c}_{11}=E$ and $c_{55}=E/[2(1+\nu)]$ for isotropic materials, where *E* is the Young's modulus and ν the Poisson's ratio.

DISPLACEMENT ASSUMPTIONS AND FORCES

According to the first-order shear deformation theory, the displacements in bender elements are assumed as

$$u_z(x,z,t)=w(x,t),\ u_x(x,z,t)=-z\psi(x,t),\tag{5}$$

where *w* is the displacement of the neutral axis, and ψ is the bending rotation as shown in Fig.2.

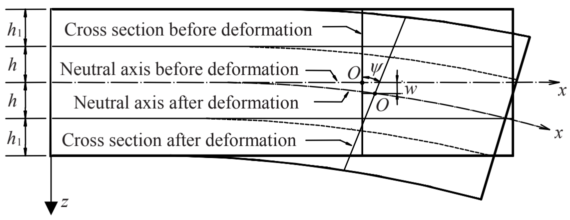

Fig.2 Piezoelectric bender element: coordinates and geometry

In general, the electric potential can be associated with the applied electric potential on the electrodes and the induced electric potential in the piezoelectric layer. In consideration of the poling directions and functions of bender elements, we propose the following functions:

$$\phi_m(x,z,t)=G(x,z,t)+\varphi(x,z,t) \\ =g(z)V_m(x,t)+f(z)\Phi_m(x,t), \quad (m=A, B), \tag{6}$$

where $V_m(x,t)$ is the amplitude at surfaces of the external applied voltage $G(x,z,t)$ (where subscripts 'A' and 'B' denote the top and bottom piezoelectric layer, respectively), and $g(z)$ is the through-the-thickness distribution of $G(x,z,t)$, which is well acknowledged as a linear distribution; $\Phi_m(x,t)$ is the amplitude of induced electric potential $\varphi(x,z,t)$ on the midline of piezoelectric layers, and $f(z)$ is the corresponding through-the-thickness distribution. To satisfy the Maxwell equation in closed circuit conditions, the induced electric potential should be in quadratic shape. Therefore $g(z)$ and $f(z)$ are proposed as (Wang *et al*., 2001; Ding and Jiang, 2005):

$$g(z)=\begin{cases}-(z+h)/h_1, & z\subset A;\\ (z-h)/h_1, & z\subset B,\end{cases} \tag{7a}$$

$$f(z)=\begin{cases}1-[(z+h+h_1/2)/(h_1/2)]^2, & z\subset A;\\ 1-[(z-h-h_1/2)/(h_1/2)]^2, & z\subset B.\end{cases} \tag{7b}$$

Substituting Eqs.(5) and (6) into Eqs.(2) and (3) yields the stress and electric displacement components in piezoelectric layers,

$$\sigma_x^{\mathrm{p}}=\begin{cases}\tilde{c}_{11}\left(-z\dfrac{\partial\psi}{\partial x}\right)-\tilde{e}_{31}\left[8\dfrac{z+h+h_1/2}{h_1^2}\Phi_A+\dfrac{1}{h_1}V_A\right], \\ \qquad z\subset A;\\ \tilde{c}_{11}\left(-z\dfrac{\partial\psi}{\partial x}\right)-(-1)^i\tilde{e}_{31}\left[8\dfrac{z-h-h_1/2}{h_1^2}\Phi_B-\dfrac{1}{h_1}V_B\right], \\ \qquad z\subset B,\end{cases} \tag{8a}$$

$$\tau_{xz}^{\mathrm{p}}=\begin{cases}-e_{15}\left\{-\left[1-\left(\dfrac{z+h+h_1/2}{h_1/2}\right)^2\right]\dfrac{\partial\Phi_A}{\partial x}+\dfrac{z+h}{h_1}\dfrac{\partial V_A}{\partial x}\right\} \\ \qquad +c_{55}\left(-\psi+\dfrac{\partial w}{\partial x}\right), \quad z\subset A;\\ -(-1)^i e_{15}\left\{-\left[1-\left(\dfrac{z-h-h_1/2}{h_1/2}\right)^2\right]\dfrac{\partial\Phi_B}{\partial x} \right. \\ \qquad \left. -\dfrac{z-h}{h_1}\dfrac{\partial V_B}{\partial x}\right\}+c_{55}\left(-\psi+\dfrac{\partial w}{\partial x}\right), \quad z\subset B,\end{cases} \tag{8b}$$

$$D_x=\begin{cases}\varepsilon_{11}\left\{-\left[1-\left(\dfrac{z+h+h_1/2}{h_1/2}\right)^2\right]\dfrac{\partial\Phi_A}{\partial x}+\dfrac{z+h}{h_1}\dfrac{\partial V_A}{\partial x}\right\} \\ \qquad +e_{15}\left(-\psi+\dfrac{\partial w}{\partial x}\right), \quad z\subset A;\\ \varepsilon_{11}\left\{-\left[1-\left(\dfrac{z-h-h_1/2}{h_1/2}\right)^2\right]\dfrac{\partial\Phi_B}{\partial x}-\dfrac{z-h}{h_1}\dfrac{\partial V_B}{\partial x}\right\} \\ \qquad +(-1)^i e_{15}\left(-\psi+\dfrac{\partial w}{\partial x}\right), \quad z\subset B,\end{cases} \tag{8c}$$

$$D_z=\begin{cases}\tilde{e}_{31}\left(-z\dfrac{\partial\psi}{\partial x}\right)+\tilde{\varepsilon}_{33}\left[8\dfrac{z+h+h_1/2}{h_1^2}\Phi_A+\dfrac{1}{h_1}V_A\right], \\ \qquad z\subset A;\\ (-1)^i\tilde{e}_{31}\left(-z\dfrac{\partial\psi}{\partial x}\right)+\tilde{\varepsilon}_{33}\left[8\dfrac{z-h-h_1/2}{h_1^2}\Phi_B-\dfrac{1}{h_1}V_B\right], \\ \qquad z\subset B.\end{cases} \tag{8d}$$

The stress components in the elastic layer can be obtained similarly

$$\sigma_x^{\mathrm{e}}=-Ez\frac{\partial\psi}{\partial x}, \tag{9a}$$

$$\tau_{xz}^{\mathrm{e}}=\frac{E}{2(1+\nu)}\left(-\psi+\frac{\partial w}{\partial x}\right). \tag{9b}$$

Then the shear force Q and moment M can be expressed as

$$M_x=\int_{-h-h_1}^{h+h_1} z\sigma_x\mathrm{d}z=b_{12}\frac{\partial\psi}{\partial x}+b_{13}\left[\Phi_A+(-1)^i\Phi_B\right]+ \\ b_{14}\left[V_A+(-1)^iV_B\right], \tag{10}$$

$$Q_x=\int_{-h-h_1}^{h+h_1}\tau_{xz}\mathrm{d}z=b_{21}\frac{\partial w}{\partial x}+b_{23}\frac{\partial}{\partial x}\left[\Phi_A+(-1)^i\Phi_B\right]+ \\ b_{24}\frac{\partial}{\partial x}\left[V_A+(-1)^iV_B\right]+b_{22}\psi, \tag{11}$$

where

$$b_{12}=-2Eh^3/3-2(\overline{c}_{11}-\overline{c}_{13}^2/\overline{c}_{33})[(h+h_1)^3-h^3]/3,$$

$$b_{13}=-\left(\overline{e}_{31}-\frac{\overline{c}_{13}}{\overline{c}_{33}}\overline{e}_{33}\right) \\ \cdot\left\{\frac{(h+h_1)^3-h^3}{3}+\frac{h+h_1/2}{2}\left[h^2-(h+h_1)^2\right]\right\}\frac{8}{h_1^2},$$

$$b_{14}=-\left(\bar{e}_{31}-\frac{\bar{c}_{13}}{\bar{c}_{33}}\bar{e}_{33}\right)\frac{h^2-(h+h_1)^2}{2h_1},$$

$$b_{21}=-b_{22}=2k(Gh+c_{55}h_1),\ b_{23}=\frac{2h_1}{3}e_{15},\ b_{24}=\frac{h_1}{2}e_{15}. \tag{12}$$

Since the transverse shear strain calculated from Eq.(5) merely is a constant and represents the value of the neutral axis, a shear coefficient k=8/9 is introduced into b_{21} and b_{22} in Eq.(11) to account for the nonlinear distribution according to FSDT (Timoshenko, 1922).

BEAM EQUATIONS OF BENDER ELEMENTS

Multiplying the first equation of Eq.(1) by z, integrating over the cross section, and making use of Eqs.(5)~(6) and other stress components, one obtains

$$-b_{21}\frac{\partial w}{\partial x}+\left(b_{12}\frac{\partial^2}{\partial x^2}-b_{22}-b_{42}\frac{\partial^2}{\partial t^2}\right)\psi+(b_{13}-b_{23})$$

$$\cdot\frac{\partial}{\partial x}\left[\Phi_A+(-1)^i\Phi_B\right]=m+(b_{24}-b_{14})\frac{\partial}{\partial x}\left[V_A+(-1)^iV_B\right], \tag{13}$$

$$-\left(b_{21}\frac{\partial^2}{\partial x^2}-b_{43}\frac{\partial^2}{\partial t^2}\right)w-b_{22}\frac{\partial\psi}{\partial x}-b_{23}$$

$$\cdot\frac{\partial^2}{\partial x^2}\left[\Phi_A+(-1)^i\Phi_B\right]=p+b_{24}\frac{\partial^2}{\partial x^2}\left[V_A+(-1)^iV_B\right], \tag{14}$$

where m and p are the external couple and force per unit length respectively, and

$$b_{42}=-2\left[\frac{h^3}{3}\rho+\rho^{\mathrm{p}}\frac{(h+h_1)^3-h^3}{3}\right],$$
$$b_{43}=2(\rho h+\rho^{\mathrm{p}}h_1), \tag{15}$$

where ρ and ρ^{p} are the densities of elastic and piezoelectric layer respectively.

The satisfaction of Maxwell equation of piezoelectric layers can be ensured approximately in a weighted sense by integration over the cross section, namely

$$\int_{-h-h_1}^{-h}\left(\frac{\partial D_x}{\partial x}+\frac{\partial D_z}{\partial z}\right)\mathrm{d}z+\int_{h}^{h+h_1}\left(\frac{\partial D_x}{\partial x}+\frac{\partial D_z}{\partial z}\right)\mathrm{d}z=0. \tag{16}$$

Substituting the electric displacements D_x and D_z into Eq.(16) yields

$$2b_{31}\frac{\partial^2 w}{\partial x^2}+2b_{32}\frac{\partial\psi}{\partial x}+\left(b_{33}\frac{\partial^2}{\partial x^2}+b_{35}\right)\left[\Phi_A+(-1)^i\Phi_B\right]$$

$$=b_{34}\frac{\partial^2}{\partial x^2}\left[V_A+(-1)^iV_B\right], \tag{17}$$

where

$$b_{31}=ke_{15}h_1,\ b_{32}=-h_1[ke_{15}+\tilde{e}_{31}],\ b_{33}=-2h_1\varepsilon_{11}/3,$$
$$b_{34}=-h_1\varepsilon_{11}/2,\ b_{35}=8\tilde{\varepsilon}_{33}/h_1. \tag{18}$$

For the sensor function, the piezoelectric layers are in open circuit and the electric potentials on the outer electrodes are non-zero and unknown, so that D_z =0 on the outer surfaces. According to Eq.(8d), it is readily obtained

$$b_{44}\frac{\partial\psi}{\partial x}+b_{45}\Phi_A+b_{46}V_A=0, \tag{19a}$$

$$b_{44}\frac{\partial\psi}{\partial x}+(-1)^ib_{45}\Phi_B+(-1)^ib_{46}V_B=0, \tag{19b}$$

where

$$b_{44}=\tilde{e}_{31}(h+h_1),\ b_{45}=-4\tilde{\varepsilon}_{33}/h_1,\ b_{46}=\tilde{\varepsilon}_{33}/h_1. \tag{20}$$

Eqs.(13), (14), (17) and (19) give the governing equations of piezoelectric sandwich beam. For series arrangement with opposite poling directions, i=1 and the external voltage is applied antisymmetrically (i.e., V_B=$-V_A$, Φ_B=$-\Phi_A$). For parallel type with identical poling directions, i=2 and the external voltage is applied symmetrically (i.e., V_B=V_A, Φ_B=Φ_A). Hence Eqs.(13), (14), (17) and (19) can be reduced to

$$-b_{21}\frac{\partial w}{\partial x}+\left(b_{12}\frac{\partial^2}{\partial x^2}-b_{22}-b_{42}\frac{\partial^2}{\partial t^2}\right)\psi$$

$$+2(b_{13}-b_{23})\frac{\partial\Phi_A}{\partial x}+2(b_{14}-b_{24})\frac{\partial V_A}{\partial x}=m, \tag{21}$$

$$-\left(b_{21}\frac{\partial^2}{\partial x^2}-b_{43}\frac{\partial^2}{\partial t^2}\right)w-b_{22}\frac{\partial\psi}{\partial x}-2b_{23}\frac{\partial^2\Phi_A}{\partial x^2}$$

$$-2b_{24}\frac{\partial^2 V_A}{\partial x^2}=p, \tag{22}$$

$$b_{31}\frac{\partial^2 w}{\partial x^2}+b_{32}\frac{\partial \psi}{\partial x}+\left(b_{33}\frac{\partial^2}{\partial x^2}+b_{35}\right)\Phi_A+b_{34}\frac{\partial^2 V_A}{\partial x^2}=0, \tag{23}$$

$$b_{44}\frac{\partial \psi}{\partial x}+b_{45}\Phi_A+b_{46}V_A=0. \tag{24}$$

Obviously, there is no fundamental difference between the analyses of series and parallel types of bender elements, since the governing equations are the same. The main difference lies in the profile directions of electric variables.

SOLUTIONS FOR SIMPLY SUPPORTED BENDER ELEMENTS

Assume m=0, and express the uniform load p as sinusoidal series as follows

$$\begin{aligned} p(x,t) &= \sum_{n=1}^{\infty}\left\{\frac{2p}{n\pi}[1-(-1)^n]\right\}\sin(n\pi x/l)\,\mathrm{e}^{\mathrm{j}\omega_n t} \\ &\triangleq \sum_{n=1}^{\infty}P_n\sin(n\pi x/l)\mathrm{e}^{\mathrm{j}\omega_n t}, \end{aligned} \tag{25}$$

where j is a purely imaginary unit.

To satisfy the simply-supported boundary conditions, w=0, σ_x=0 and Φ=0, the displacement w, rotation ψ, electric potential Φ and surface voltage can be expressed as follows:

$$\begin{Bmatrix} w(x,t) \\ \Phi(x,t) \\ V(x,t) \end{Bmatrix} = \sum_{n=1}^{\infty}\begin{Bmatrix} W_n \\ \Phi_n \\ V_n \end{Bmatrix}\sin(n\pi x/l)\,\mathrm{e}^{\mathrm{j}\omega_n t}, \tag{26a}$$

$$\psi(x,t)=\sum_{n=1}^{\infty}\Psi_n\cos(n\pi x/l)\,\mathrm{e}^{\mathrm{j}\omega_n t}. \tag{26b}$$

Substituting Eqs.(25) and (26) into Eqs.(21)~(24), yields

$$\begin{bmatrix} a_{11} & a_{12} & a_{13} & a_{14} \\ a_{21} & a_{22} & a_{23} & a_{24} \\ a_{31} & a_{32} & a_{33} & a_{34} \\ a_{41} & a_{42} & a_{43} & a_{44} \end{bmatrix}\begin{Bmatrix} W_n \\ \Psi_n \\ \Phi_n \\ V_n \end{Bmatrix} = \begin{Bmatrix} 0 \\ P_n \\ 0 \\ 0 \end{Bmatrix}, \tag{27}$$

where

$$\begin{aligned} & a_{11}=-b_{21}n\pi/l,\ a_{12}=-b_{12}(n\pi/l)^2-b_{22}+b_{42}\omega_n^2, \\ & a_{13}=2(b_{13}-b_{23})n\pi/l,\ a_{14}=-2(b_{24}-b_{14})n\pi/l, \\ & a_{21}=b_{21}(n\pi/l)^2-b_{43}\omega_n^2,\ a_{22}=b_{22}n\pi/l, \\ & a_{23}=2b_{23}(n\pi/l)^2,\ a_{24}=2b_{24}(n\pi/l)^2, \\ & a_{31}=-b_{31}(n\pi/l)^2,\ a_{32}=-b_{32}n\pi/l, \\ & a_{33}=-b_{33}(n\pi/l)^2+b_{35},\ a_{34}=-b_{34}(n\pi/l)^2, \\ & a_{41}=0,\ a_{42}=-b_{44}n\pi/l,\ a_{43}=b_{45},\ a_{44}=b_{46}. \end{aligned} \tag{28}$$

To check the performance of the present solutions for sensor function, two key issues are to be examined based on Eq.(27) and the exact 2D solutions: the first one is the accuracy of electric potential under applied static force, because in practical tests the output voltage is the main measurement; the second one is the free vibration characteristics, based on which forced vibration analysis could be performed. Note that the exact 2D solution is obtained according to state space approach (SSA) (Zhou, 2007; Lee and Jiang, 1996). The length of the bender element for calculation is L=1 m, the piezoelectric material is PZT-5A, and the metal shim is copper (Zhou *et al.*, 2005a).

Static responses of sensor function

The static responses could be obtained by setting ω_n=0 in Eqs.(25)~(28). A uniform surface force density, p=1 N/m^2, is applied to the element with open circuit. Fig.3a and 3b show the electric potential at x=0.5L for parallel and series types respectively, where the thickness-to-length ratio $2(h+h_1)/L$ is 0.2. As shown in Fig.3, the present solution compares with the 2D solution very well, with the maximum error of 5.6% on the outer surfaces.

Free vibration of sensor function

For free vibration analysis, the right-hand side of Eq.(27) should vanish. Then solving Eq.(27) gives the frequencies of flexural vibrations for a given n. Fig.4 shows the frequency ratio ω_n/ω_n^* of the first 5 modes for different values of thickness-to-length ratio R, where ω_n^* is the 2D solution. It is found from Fig.4 that the accuracy of the present model is very high, with error being less than 2% even as R=0.5.

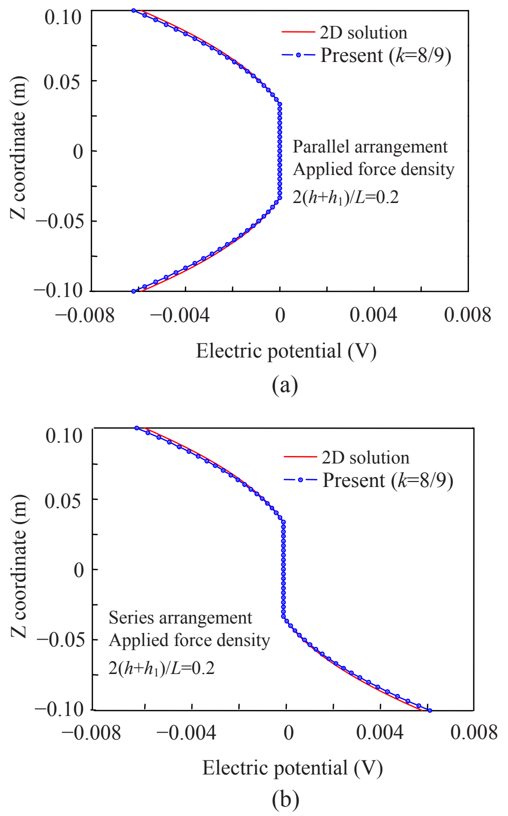

Fig.3 Profile of electric potential under applied force density. (a) Parallel; (b) Series

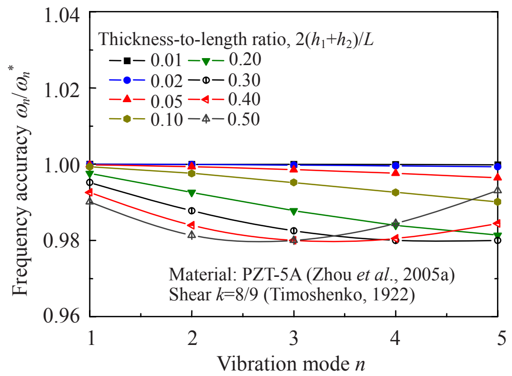

Fig.4 Frequencies predicted by the present model (open circuit)

CONCLUSION

In the present study, the piezoelectric bender elements are investigated and an analytical sandwich beam model is established based on the first-order shear deformation theory (FSDT). The model combines an equivalent single-layer approach for the mechanical displacements with a layerwise assumption for the electric potential, and introduces shear coefficient to account for the nonlinear distribution of transverse shear strain on the cross-section. Static and free vibration analyses of simply supported bender elements are presented for the sensor function. The comparison with 2D solutions proves the accuracy of the present model. This work offers an efficient model for sensor function analyses of bender elements.

References

Arulnathan, R., Boulanger, R.W., Riemer, M.F., 1998. Analysis of bender element tests. *Geotechnical Testing Journal*, **21**(2):120-131. [doi:10.1520/GTJ10750J]

Ding, H.J., Jiang, A.M., 2005. Polynomial solutions to piezoelectric beams (I)—several exact solutions. *Applied Mathematics and Mechanics*, **26**(9):1107-1114. [doi:10.1007/BF02507718]

Ding, H.J., Wang, G.Q., Chen, W.Q., 1997. Green's functions for a two-phase infinite piezoelectric plane. *Proceedings of the Royal Society of London* (*A*), **453**(1966):2241-2257. [doi:10.1098/rspa.1997.0120]

Fernandes, A., Pouget, J., 2003. Analytical and numerical approaches to piezoelectric bimorph. *International Journal of Solids and Structures*, **40**(17):4331-4352. [doi:10.1016/S0020-7683(03)00222-1]

Lau, C.W.H., Lim, C.W., Leung, A.Y.T., 2005. A variational energy approach for electromechanical analysis of thick piezoelectric beam. *Journal of Zhejiang University SCIENCE*, **6A**(9):962-966. [doi:10.1631/jzus.2005.A0962]

Lee, J.S., Jiang, L.Z., 1996. Exact electroelastic analysis of piezoelectric laminae via state space approach. *International Journal of Solids and Structures*, **33**(7):977-990. [doi:10.1016/0020-7683(95)00083-6]

Lee, J.S., Santamarina, J.C., 2005. Bender elements: performance and signal interpretation. *Journal of Geotechnical and Geoenvironmental Engineering, ASCE*, **131**(9):1063-1070. [doi:10.1061/(ASCE)1090-0241(2005)131:9(1063)]

Leong, E.C., Yeo, S.H., Rahardjo, H., 2005. Measuring shear wave velocity using bender elements. *Geotechnical Testing Journal*, **28**(5):488-498. [doi:10.1520/GTJ12196]

Timoshenko, S.P., 1922. On the transverse vibrations of bars of uniform cross section. *Philosophical Magazine*, **43**(6):125-131.

Wang, Q., Quek, S.T., Sun, C.T., Liu, X., 2001. Analysis of piezoelectric coupled circular plate. *Smart Materials and Structures*, **10**(2):229-239. [doi:10.1088/0964-1726/10/2/308]

Zhou, Y.G., 2007. Shear Wave Velocity-based Characterization of Soil Structure and its Effects on Dynamic Behavior. Ph.D Thesis, Zhejiang University (in Chinese).

Zhou, Y.G., Chen, Y.M., 2005. Influence of seismic cyclic loading history on small strain shear modulus of saturated sands. *Soil Dynamics and Earthquake Engineering*, **25**(5):341-353. [doi:10.1016/j.soildyn.2005.03.001]

Zhou, Y.G., Chen, Y.M., 2007. Laboratory investigation on assessing liquefaction resistance of sandy soils by shear wave velocity. *Journal of Geotechnical and Geoenvironmental Engineering, ASCE*, **133**(8):959-972. [doi:10.1061/(ASCE)1090-0241(2007)133:8(959)]

Zhou, Y.G., Chen Y.M., Ding, H.J., 2005a. Analytical solutions to piezoelectric bimorphs based on improved FSDT beam model. *Smart Structures and Systems*, **1**(3):309-324.

Zhou, Y.G., Chen Y.M., Ding, H.J., 2005b. Analytical modelling and free vibration analysis of piezoelectric bimorphs. *Journal of Zhejiang University SCIENCE*, **6A**(9):938-944. [doi:10.1631/jzus.2005.A0938]

Zhou, Y.G., Chen, Y.M., Ding, H.J., 2007. Analytical modeling of sandwich beam for piezoelectric bender elements. *Applied Mathematics and Mechanics*, **28**(12):1411-1416.